THE ASTROPHYSICAL JOURNAL, 407:14–21, 1993 April 10

THE Im/dE,N MIXED MORPHOLOGY DWARF ESO 359-G29 AS A PROBE OF A MASSIVE HALO IN NGC 1532

ALLAN SANDAGE
The Observatories of the Carnegie Institution of Washington, 813 Santa Barbara Street, Pasadena, CA 91101-1292
AND
EDWARD FOMALONT
National Radio Astronomy Observatory,[1] Edgemont Road, Charlottesville, VA 22903-2475
Received 1991 July 7; accepted 1992 October 6

ABSTRACT

A low surface brightness dwarf, ESO 359-G29, in the neighborhood of the NGC 1532/31 pair, has the morphology of an early-type dE,N/dS0,N nucleated dwarf in yellow and red wavelengths, but shows an Sm or Im late-type morphology in the blue. This mixed morphology is similar to that of the prototype example NGC 4286, companion to NGC 4278. VLA observations of H I, however, show that ESO 359-G29 has a typical dwarf hydrogen content unlike NGC 4286 which is hydrogen depleted.

The velocity distribution in NGC 1532 has also been determined from VLA observations of H I. At a distance of 64 kpc from the galaxy, the rotational velocity is 250 km s^{-1}, and it is still slowly increasing with distance. The unique geometry and relative motion of the ESO 356-G29 and NGC 1532 configuration suggest that ESO 359-G29 is in a polar orbit of NGC 1532 at a radius of 83 kpc and a velocity of 300 km s^{-1}. From these velocities, we derive a total mass of NGC 1532 of $1.7 \times 10^{12}\ M_{\odot}$. The halo radius, although uncertain, is probably not larger than 70 kpc. The disk component contains less than 10% of the total mass and its mass-to-light ratio is in range of 2.5–7. The mass-to-light ratio of the halo material is greater than 80.

Subject headings: galaxies: fundamental parameters — galaxies: individual (ESO 359-G29) — galaxies: kinematics and dynamics — galaxies: structure

1. INTRODUCTION

In the course of reclassifying the Shapley-Ames galaxies for the Carnegie Atlas of Bright Galaxies (Sandage & Bedke 1993), several unusual mixed morphology Im/dE,N dwarf galaxies were noted. Such mixed morphology systems have the potential to help in the understanding of the origin and evolution of dE galaxies.

Two such galaxies, NGC 4286, companion to NGC 4278 (E1), and NGC 3377A, companion to NGC 3377, were noted and discussed by Sandage & Hoffman (1991, hereafter SH). Images of NGC 4286 in the red show a classical morphology of a low surface brightness, nucleated dwarf E or S0 galaxy. Images in the blue, however, show a small but finite rate of recent star formation and suggestion of a weak spiral pattern. The H I and total mass in NGC 4286, deduced from the 21 cm hydrogen line, show an abnormally low cold hydrogen–to–total mass ratio of 0.006. In addition, the distance independent ratio of hydrogen mass-to-optical luminosity of 0.07 is intermediate between that of S0 and Sa galaxies.

In the course of the same program, a similar mixed morphology dwarf ESO 359-G29 (Lauberts 1982) was found in the neighborhood of the interacting galaxy pair NGC 1532/31. Red and yellow images were made to determine the properties of ESO 359-G29. The optical properties of this Im/dE, N dwarf and the interacting galaxy pair are set out in § 2. The VLA observations to determine the H I distribution in ESO 359-G29 and NGC 1532/31 are described in § 3. The results have produced the unexpected by-product that ESO 359-G29 is rotating around the interacting pair NGC 1532/31. The comparison of ESO 359-G29 with NGC 4286 and other mixed galaxy types is given in § 4. In § 5 we have estimated the amount of dark matter in the halo of NGC 1532 from its hydrogen distribution and kinematics and from the orbital velocity of ESO 359-G29. Conclusions are given in § 6.

[1] The National Radio Astronomy Observatory is operated by Associated Universities, Inc., under cooperative agreement with the National Science Foundation.

2. OPTICAL MORPHOLOGY

2.1. *ESO 359-G29*

Figure 1 (Plate 1) shows the extended field containing the interesting galaxy pair NGC 1531 and NGC 1532 (the dominant galaxy) and the dwarf ESO 359-G29, located 13′ southeast of the major pair. The reproduction is from a yellow (103a-D + GG495) plate taken with the 2.5 m du Pont telescope at Las Campanas. ESO 359-G29 is of low surface brightness and has a sharp object at the center that is unresolved at 0″.7 resolution, similar to the nuclei of classical nucleated dE galaxies but rare in Sm and Im dwarfs. Furthermore, the image on the yellow plate is nearly smooth, resembling closely the morphology of normal dE, N or dS0 forms seen, for example, in the Virgo Cluster Atlas of Dwarfs (Sandage & Binggelli 1984). The image is still more featureless, and with the nucleus even more pronounced, on the red plate (103a-E + GG610), also taken at Las Campanas (not shown here). We were, therefore, astonished to see evidence of recent star formation and a weak but definite spiral pattern in the blue image where the morphological type is Sm or Im.

Enlarged images from the yellow and the blue (103-a-O + GG385) plate are shown in Figures 2*a* and 2*b* (Plate 2), respectively. The differences in the morphology between the yellow and the blue images for ESO 359-G29 are remarkably similar to those for NGC 4286 (SH, Fig. 2), suggesting a similar rare mixed morphology between dwarf Sm/Im and dE types.

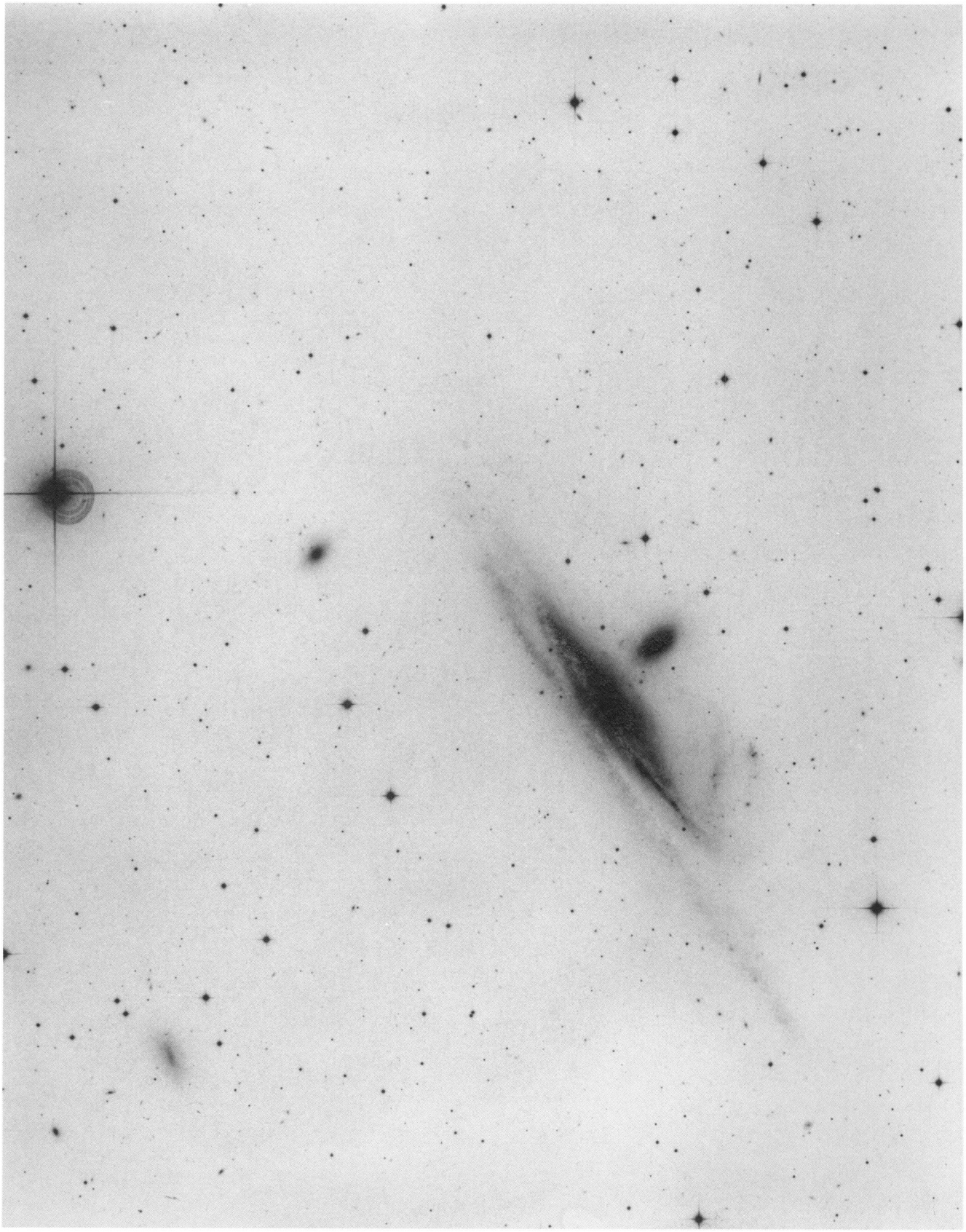

FIG. 1.—Wide-angle view of the interacting Shapely-Ames pair NGC 1532 Sbc(s)I(tides?) and NGC 1531 (Amorphous) to the right of the center. The low surface brightness dwarf companion of mixed morphology, ESO 359-G29, is at the lower left. The high surface brightness SB0 galaxy IC 2401 to the left and slightly above NGC 1532/31 is of unknown redshift. The reproduction is from a yellow (103-aD + GG495) plate taken on 1981 October 27/28, with the du Pont reflector at Las Campanas. North is at the top; east to the left.

PLATE 2

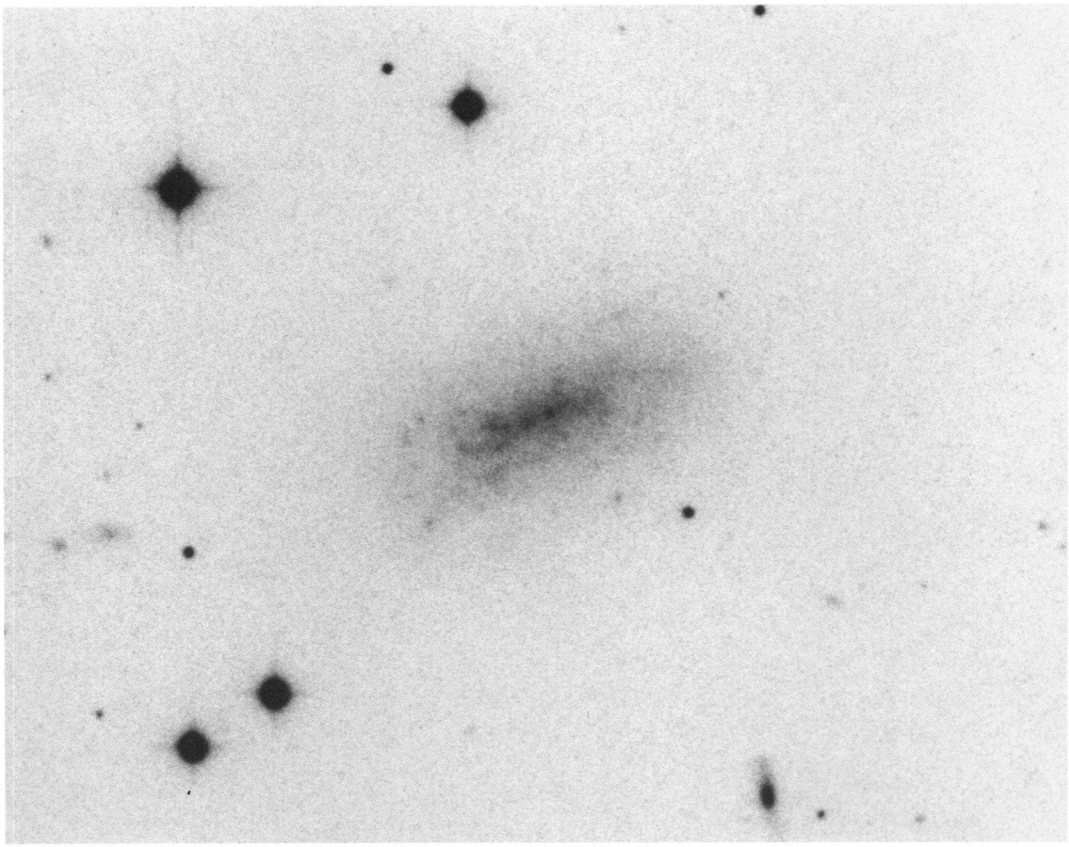

FIG. 2*a*

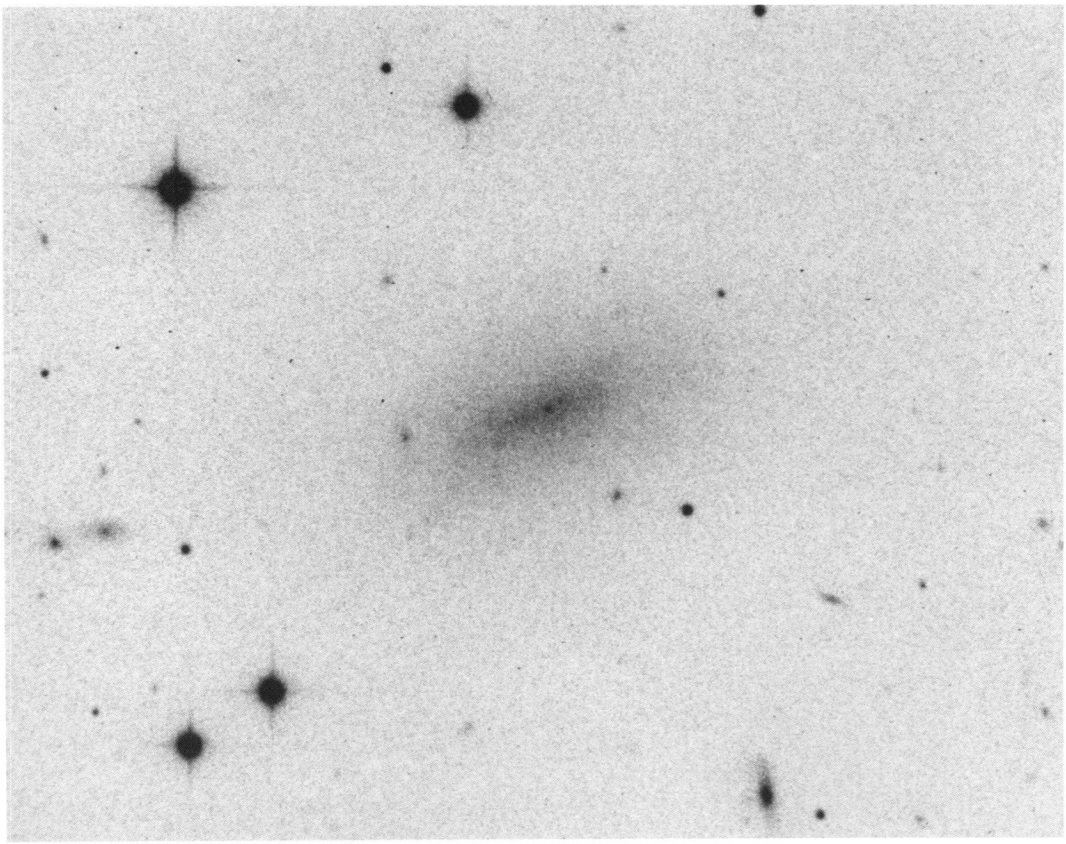

FIG. 2*b*

FIG. 2.—(*a*) ESO 359-G29 from the same yellow plate used for Fig. 1. North is the left; west is up. (*b*) Image from a blue plate (103-aO + GG385) taken at Las Campanas on 1979 February 21/22.

The photometric properties of ESO 359-G29, as listed by Lauberts & Valentijn (1989, hereafter LV) are as follows:

1. The total magnitude is $B_T = 14.8$. At the distance of 22 Mpc (adopted from NGC 1532, see below), the corresponding absolute magnitude is $M_{B(T)} = -16.9$.

2. The circle containing half of the light has a diameter of 45″, and 90% of the light is contained within a major axis diameter of 100″.

3. The resulting effective surface brightness is $SB_e = 23.5B$ mag (arcsec)$^{-2}$, conforming to the mean SB–absolute magnitude relation for dE dwarfs (Binggeli, Sandage, & Tarenghi 1984; Ferguson & Sandage 1988; Sandage & Perelmuter 1990, Fig. 11) at $M_B = -16.9$.

4. The flattening ratio obtained from Figures 2*a* and 2*b* is consistent with $b/a = 0.42$, listed by LV.

5. The $B_T - R_T$ color from LV is 0.63, intermediate between the colors for dE and Im dwarfs as expected, given the prominent evidence for blue star formation in Figure 2*b*.

Spurred by the optical similarities with NGC 4286 where very weak H I has been detected (SH), we have searched for 21 cm H I in ESO 359-G29.

2.2. *NGC 1532/31*

The galaxy pair, consisting of NGC 1532, a dominant Sbc(s) with possible tidal distortions, and NGC 1531, an interacting less massive amorphous type, has been well studied. A summary of the photometric properties (taken from RSA and LV) follows:

1. The heliocentric redshift of NGC 1532 is 1208 ± 10 km s^{-1}. Correcting to the centroid velocity of the local group gives a redshift of 1105 km s^{-1}. Hence, we adopt a distance of 22 Mpc using $H_0 = 50$ km s^{-1} Mpc^{-1}. An angular scale of 10″ corresponds to a linear scale of 1.07 kpc.

2. For NGC 1532 and 1531, respectively, the total magnitudes are $B_{(T)} = 11.5$ and 12.8; the corresponding absolute magnitudes (corrected for internal and external absorption) are $M_{B(T)} = -21.0$ and -18.9.

3. The disk of NGC 1532 has a major axis diameter of 292″. The flattening is 0.28 and the inclination is 77° (Huchtmeier & Richter 1989).

4. The surface brightness averaged over 10″ of the center of the galaxy is $SB_e = 19.8B$ mag (arcsec)$^{-2}$.

5. The $B_T - R_T$ color from LV is 2.04.

3. EMISSION FROM THE GALAXIES

3.1. *The VLA Observations*

Our initial assumption of the frequency range over which to make the search for H I radiation was based on considering ESO 359-G29 to be a companion of the NGC 1532/31 pair. All known dE galaxies are either in great clusters such as Virgo, Fornax, and Coma (Reaves 1956; Caldwell 1983; Binggeli, Sandage, & Tammann 1985; Ferguson 1989; Thompson & Gregory 1992), in smaller groups (Ferguson & Sandage 1990), or as companions to massive single parents (Vader & Sandage 1991). Free floaters in the general field are believed to be nonexistent.

Since the redshift of NGC 1532 is v(helio) $= 1208 \pm 10$ km s^{-1} (Sandage & Tammann 1987; Huchtmeier & Richter 1989; Bottinelli et al. 1990), we searched for 21 cm H I emission in the range of velocities between 860 and 1500 km s^{-1}, corresponding to a 3.1 MHz frequency range. The search was made with the C/D configuration at the VLA with an angular resolution of 40″ for a source at this declination. The field of view of radius 16′ to half-power sensitivity was centered between NGC 1532 and ESO 359-G29, each of which was 6.′5 from the field center. The loss in sensitivity at these positions compared with that at the field center is about 10%. Using the spectral line correlator, images were made simultaneously at 63 velocity channels, each with a width of 10.3 km s^{-1} or 48.8 KHz.

We integrated on the galaxy field for a total of 4 hr, alternating observations of the calibrator source 0451−282 for a period of 2 minutes every 30 minutes. All positions are tied to the assumed position of the calibrator ($\alpha = 04^h51^m15^s.127$; $\delta = -28°12'29''.39$) with an accuracy of 0″.1. From a 6 minute integration on the strong source 3C 48 we determined the flux density scale of the data (assuming a flux density of 16.0 Jy at 1414 MHz) and the relative amplitude and phase across the 63 velocity channels with an accuracy of 1% and 2°, respectively.

Images were made using the AIPS software. The considerable H I emission from the galaxy pair NGC 1532 was very extended so the MEM deconvolution algorithm (Cornwell & Evans 1985) was used to obtain good quality images for all 63 velocity channels. The sensitivity of the images were limited by receiver noise which was approximately 1.5 mJy in 40″ or about 10 K brightness temperature.

3.2. *The* H I *Emission from ESO 359-G29*

ESO 359-G29 was detected in 21 cm emission between the heliocentric velocities of 860 and 954 km s^{-1}, near the low end of our search window. There was no continuum emission from the galaxy outside this velocity range to a 2 σ level of 0.5 mJy. The most surprising feature of the detection of H I is the small redshift of ESO 359-G29 at v(helio) $= 900 \pm 10$ km s^{-1}, compared with v(helio) $= 1208 \pm 10$ km s^{-1} for NGC 1532. This suggested that ESO 359-G29 may not be gravitationally bound to NGC 1532. The emission was just resolved with 40″ resolution, and Figure 3 shows the H I profile integrated over the emission in each of the velocity channels. Because of the roll-off in sensitivity in frequency channels 61–63, the errors in the H I emission for the low velocities are large. Nevertheless it is evident that the profile is falling toward the smallest observed velocities and that the entire plateau of the velocity profile has been covered.

The integrated H I flux density, $\int S\,dv$, between $860 < v < 954$ km s^{-1}, is 1.39 ± 0.10 Jy km s^{-1}. We have estimated that additional H I emission below 860 km s^{-1}, based on the expected symmetry of the emission with velocity and position, is 0.25 ± 0.10 Jy km s^{-1}. Hence, the total H I flux density from ESO 359-G29 is 1.64 ± 0.14 Jy km s^{-1}.

Over the span of 880–930 km s^{-1} the H I centroid positions shift linearly along the major axis by about 25″ in the sense that the north side of ESO 359-G29 is receding. The inner part of the galaxy appears to be in solid body rotation (although our velocity-spatial resolution is marginal). The observed gradient corresponds to the observed profile width of ≈ 75 km s^{-1} over the major axis diameter of $\approx 50''$ for the main optical body. The H I emission also extends about 15″ perpendicular to the major axis for velocities near the center of the emission line.

3.3. *The* H I *Emission from NGC 1532*

The H I emission from NGC 1532 and its companion NGC 1531 is strong and extensive in velocity and spatial coordinates. Fortunately, the observed velocity range of 860–1500

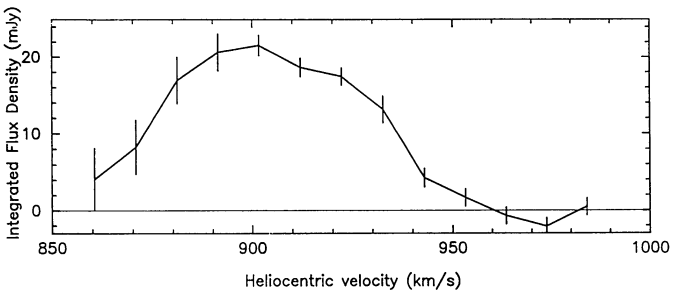

FIG. 3a

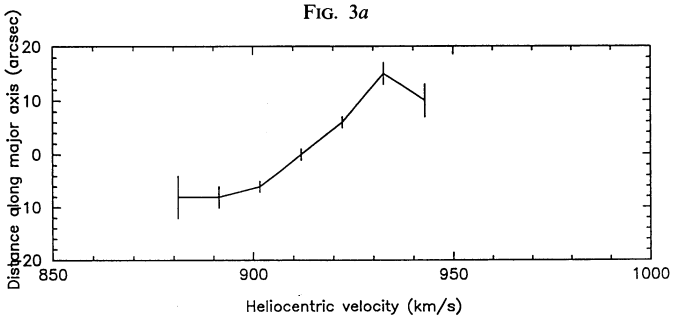

FIG. 3b

FIG. 3.—(*a*) H I profile of ESO 359-G29 from VLA observations with 10.3 km s^{-1} velocity resolution. The velocity axis shows the heliocentric values. (Velocities reduced to the frame of the centroid of the Local Group are 103 km s^{-1} smaller than heliocentric, based on precepts of the RSA). Line segments connect the integrated flux density samples each 10.3 km s^{-1} and vertical segments show the error in the measured flux density. (*b*) Rotation curve of ESO 359-G29. The mean position of the H I emission is plotted vs. heliocentric velocity. The brightest seven velocity channels between 881 and 943 km s^{-1} have sufficient signal to determine an accurate position. The ordinate scale is in arcseconds along the major axis (PA 15°, north through east) with respect to R.A.(1950) = 04^{h}10^{m}56^s.22, decl.(1950) = −33°07′22″.6. Vertical line segments indicate the error in the measured position.

km s^{-1} just does cover the total H I coming from the region. The continuum emission was obtained from the few H I free channels near the band edges and from the high-velocity channels where the H I emission is confined to the outer parts of the galaxy. Our derived continuum emission agrees with that measured by Condon (1989) for the galaxy pair.

The H I profile, with the continuum removed, is shown in Figure 4 with the full resolution of 10.3 km s^{-1}. The profile shows the typical double-horned response for a rotating galaxy. The peak near the middle velocities of the profile is associated with a star-forming region about 3′ southwest of the nucleus of NGC 1532. The integrated H I emission is 228 ± 15 Jy km s^{-1} and the average velocity of the H I is 1130 ± 14 km s^{-1}. This H I emission gives a total H I mass of 2.7 × 10^{10} $M_\odot$ The velocity spread between the two peaks is 450 km s^{-1} with a center velocity of 1195 ± 10 km s^{-1}. The total velocity spread is about 550 km s^{-1}. These velocities are in good agreement with those listed by Bottinelli et al. (1990); however, the emission is extensive and the VLA image contain about 50% more H I emission.

The detailed kinematics of the NGC 1532/31 system will be given elsewhere (Fomalont & Kristian 1992); however, the properties of the H I emission and kinematics can be summarized from the displays in Figures 5*a*, 5*b*, and 5*c*. Figure 5*a* shows a contour plot of the NGC 1532/31 pair, made from a digital representation of Figure 1. The coordinate grid was determined by measuring the positions of about 10 bright field stars which are on the PSS prints. The contour levels are not known (because of the unknown transfer functions in making the digital image from the photograph) but with the astrometry, which is accurate to 2″, a comparison of the optical features and the radio features can be made. The disk component of NGC 1532, the center of NGC 1531, and the two star-forming regions 3′ and 6′ to the southwest of the center of NGC 1532, are indicated by marks in Figure 5*a*.

The H I emission, integrated over all velocities, is shown in Figure 5*b*. For convenient correspondence with the optical field, pertinent locations are indicated by the symbols. The H I emission from NGC 1531 is much less than that from NGC 1532. Figure 5*c* gives the velocity field of the H I emission. The contour levels show the average velocity of the H I over the region with significant H I emission.

The H I emission from NGC 1532/31 has the following properties:

1. The general emission and kinematic properties are consistent with a rotating galaxy, with the maximum rotation somewhat outside of the disk component. Although the spatial resolution is relatively low, it appears that the inner disk is in solid-body rotation.
2. To the northeast the H I velocity is about 1420 km s^{-1} and a substantial amount of H I lies several arcminutes beyond the disk component.
3. To the southwest the H I velocity lies within the range 950–1050 km s^{-1} and the H I emission is more intense than that to the northeast. Much of this additional emission is associated with the star-forming region indicated in Figure 5*b*.
4. H I emission extends along the entire length of the southwest extended arm, up to 10′ (60 kpc) from the galaxy nucleus. The velocity remains at about 950 km s^{-1} and shows little change with distance from the galaxy center.
5. The weak H I emission from NGC 1531 is confined to velocities 1160–1340 km s^{-1}. The higher velocities occur to the west of this galaxy, the lower velocities to the east, and blend into that of the nuclear region of NGC 1532.

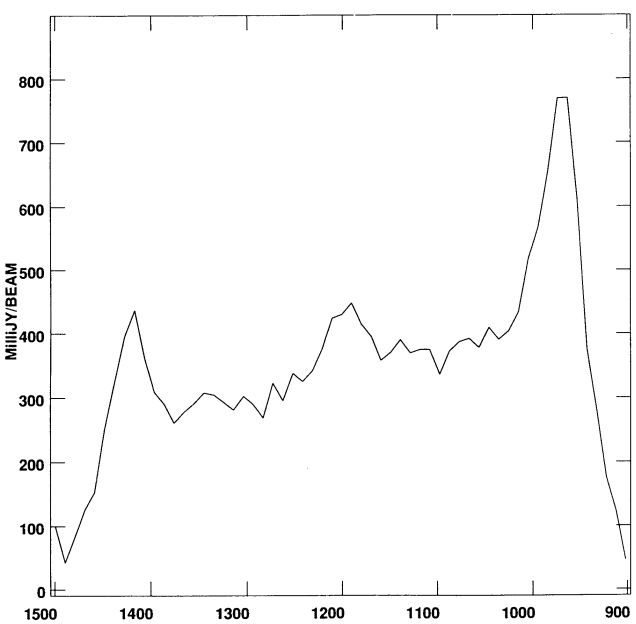

FIG. 4.—The H I profile of NGC 1532 from VLA observations with 10.3 km s^{-1} velocity resolution. The abscissa gives the heliocentric velocity, and the ordinate gives the integrated H I flux density over the galaxy in a 10.3 km s^{-1} range. The continuum emission has been subtracted.

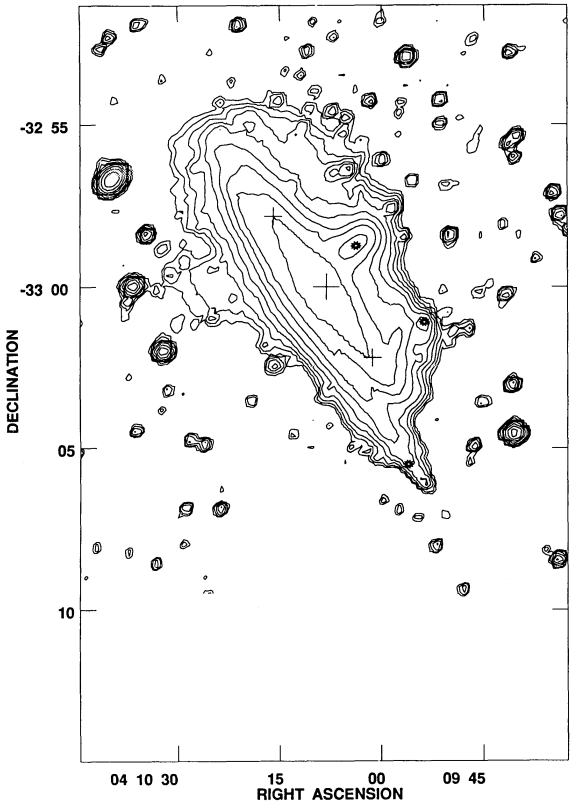

FIG. 5a

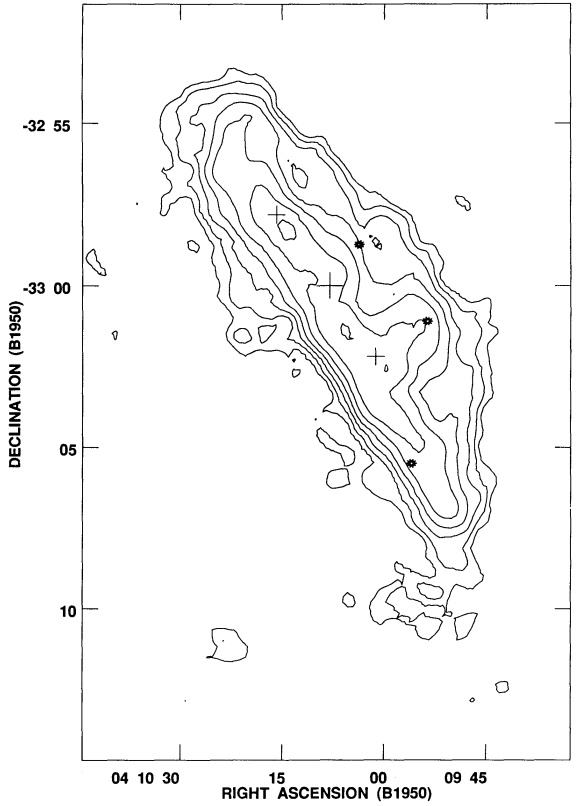

FIG. 5b

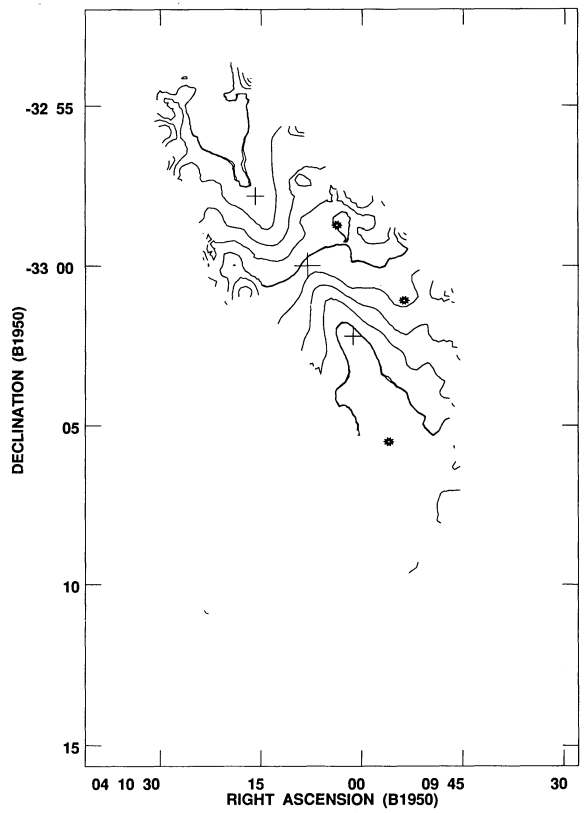

FIG. 5c

FIG. 5.—(*a*) Brightness contours of the galaxy NGC 1532 with 15″ resolution. The image in Figure 1 has been smoothed to obtain this representation. The contour levels are somewhat arbitrary, and this diagram is meant to display the major features of the galaxy in a qualitative manner. The coordinate grid is accurate to about 2″. The plus signs give the location of the nucleus (*big cross*) and the edges of the disk component (*small crosses*). The location of NGC 1531 is given by the uppermost asterisk, the star-forming region about 3′ SW of the nucleus by the middle asterisk, the last knot in the SW spiral arm by the lower asterisk. These same symbols are used in Figs. 5*b* and 5*c*. (*b*) The H I distribution, integrated over all velocities, for NGC 1532. The bottom contour level is 0.3 Jy km s^{-1}, and each contour increases by a factor of 1.58. The peak emission is 5.18 Jy km s^{-1}. The plus symbols and the circular symbols show the location of optical objects described in (*a*). (*c*) The velocity field for NGC 1532. The contours show the average velocity of the H I in the galaxy. Only regions with an integrated intensity (see [*b*]) greater than 0.4 Jy km s^{-1} are included. The contour intervals are 50 km s^{-1}, with the three bold contours at +200 km s^{-1} (*top*), 0 km s^{-1} (*middle*), −200 km s^{-1} (*bottom*) with respect to 1200 km s^{-1} at the nucleus. The sense of the galaxy rotation is that the SW part is moving toward us. The plus symbols and the circular symbols show the location of optical objects described in (*a*).

TABLE 1

PARAMETERS OF NUCLEATED DWARF GALAXIES

Parameter	ESO 359-G29	NGC 4286	NGC 3377A
R.A.(1950.0)	$04^h10^m56^s.22$	$12^h18^m11^s.2$	$10^h44^m43^s.5$
Decl.(1950.0)	$-33°07'22''.06$	$29°37'16''.0$	$14°20'07''.0$
Distance r (Mpc)	22	10	10
Optical:			
B_T	14.8	14.7	14.2
$M_{B(T)}$	−16.9	−15.3	−15.8
D_{50}	43″(4.6 kpc)	50″(2.4 kpc)	99″(4.8 kpc)
D_{25}	78″(8.3 kpc)	114″(5.5 kpc)	120″(5.8 kpc)
b/a	0.42	0.55	0.94
$L_B(L_\odot)$	9.1×10^8	2.1×10^8	3.3×10^8
$SB_B(L_\odot\ \mathrm{kpc}^{-2})$	5.5×10^7	4.6×10^7	0.7×10^7
Radio:			
v heliocentric (km s^{-1})	900 ± 10	644 ± 15	573 ± 8
Δv (km s^{-1})	90	115	60
$\int S\,dv$ (mJy km s^{-1})	1640	670	3840
$M_H(M_\odot)$	1.9×10^8	0.16×10^8	0.91×10^8
$SB_H(L_\odot\ \mathrm{kpc}^{-2})$	3.3×10^6	0.7×10^6	3.4×10^6
$M_T(M_\odot)$	2.2×10^9	2.9×10^9?	5.1×10^9?
Ratios:			
$M_H/L_B(M_\odot/L_\odot)$	0.21	0.076	0.28
M_H/M_T	0.09	0.006?	0.018?
$M_T/L_B(M_\odot/L_\odot)$	2.4	13.8?	15.4?

NOTES.—? = uncertain. $M_H/L_B = 1.34 \times 10^{-10} \times 10^{0.4B} \int S\,dv$. $M_H = 236r^2 \int S\,dv$. $M_T = 2.85 \times 10^4 D_{25}(\Delta v)^2[1 - (b/a)^2]^{-1}$.

Detailed analysis of the rotation curve of NGC 1532 is given in § 5.1.

4. COMPARISON OF ESO 359-G29 WITH NGC 4286 AND NGC 3377A

In Table 1 we have compared the measured and derived properties of the three galaxies ESO 359-G29, NGC 4286 and NGC 3377A. The data were taken from this paper, from SH (1991), from LV (1989), and from Lewis (1987). The equations used in calculating the parameters in the table are given in the notes.

The properties of these mixed morphological galaxies are as follows.

1. All three galaxies, ESO 359-G29, NGC 4286, and NGC 3377A, show nuclear star-forming regions in blue light but are relatively smooth in the yellow. They have approximately the same luminosities and angular extents.

2. Their H I masses, however, vary considerably. ESO 359-G29 has over 10 times the amount of H I compared with NGC 4286, while the H I in NGC 3377A is comparable to that in ESO 359-G29. The hydrogen mass in the Phoenix dwarf is also low, $1.5 \times 10^5\ M_\odot$ (Carignan, Demers, & Côte 1991).

3. The ratio of $M_H/L_B = 0.2$ for ESO 359-G29 is similar to the late type dwarfs in the Virgo Cluster (Hoffman et al. 1985, hereafter HHSS, Figs. 1–5) for the "bright" Im and BCD's, and the ratio rises to 0.4 for the Im types fainter than $M_B = -15$. Note also that the very low surface brightness Im dwarf of NGC 3377A with a ratio of 0.3 is typical of Sc galaxies rather than S0's. In the study of a complete sample of Shapley-Ames galaxies, Haynes et al. (1990) showed that most S0's have M_H/L_B ratios smaller than 0.01; less than 5% of their sample had a ratio greater than 0.1. Hence ESO 359-G29 is gas rich for its dE, N optical morphology in the yellow and red.

4. We have estimated the total dynamical mass in each galaxy assuming that the width of the H I profile was a measure of the rotation of the galaxy and that the radius at maximum rotation was at the 25% isophote, which is typical for a dwarf or spiral galaxy. The derived total masses are similar amongst the three galaxies at (2–5) $\times 10^9\ M_\odot$. We used the observed flattening (b/a) to determine the inclination of the galaxies. Only NGC 3377A is nearly face-on, and its mass estimate may be in error by a factor of 2.

5. The H I mass to total mass ratio, M_H/M_T, also shows the hydrogen-rich status of ESO 359-G29 (0.09) and the hydrogen-poor status of NGC 4286 (0.006), with the ratio for NGC 3377A at 0.018. The ratio of 0.1 is about that for Virgo dwarfs (HHSS, combining data from their various figures), and this again indicates the ESO 359-G29 is not hydrogen depleted.

6. The mass-to-light ratio in ESO 359-G29 of 2.4 suggests that very little dark matter is associated with this dwarf. The larger values for the other two galaxies are more suspect since the determination of their dynamical masses are uncertain. Their H I distribution has not been accurately mapped.

We conclude that the H I content of ESO 359-G29 is normal in all comparisons with the unbiased distance-limited sample of Virgo Cluster dwarfs (HHSS). There is no evidence for gas depletion of this galaxy, although a similar mixed morphology dwarf NGC 4286 is nearly depleted of H I. Perhaps ESO 359-G29 is in an earlier stage of star formation, while NGC 4286 has either converted its available source of H I into new stars, or has blown away any original gas it had by super-galactic winds made by a massive young star cluster in the manner suggested by SH—the star cluster evolving into the present nucleus. The amorphous galaxies NGC 1705 (Meurer, Freeman, & Dopita 1988; Meurer et al. 1992) and NGC 625 (Sandage & Bedke 1993, section on amorphous galaxies) are seen to presently be in this state of transformation, believed to end in a dE, N gas-poor dwarf.

5. THE HALO COMPONENT OF NGC 1532

The H I emission from NGC 1532 is extensive and has been summarized in § 3.3. A detailed analysis of H I emission and kinematics of the interacting system will be given elsewhere (Fomalont & Kristian 1993). Here we will determine the average rotational curve of NGC 1532 from the H I observations within about 10′ (63 kpc) of the galaxy. We will then suggest that ESO 359-G29 is in a polar orbit around NGC 1532 at a distance of 82 kpc permitting, in effect, the extension of the rotation curve to this distance from NGC 1532.

5.1. *The Rotation Curve of NGC 1532*

For the analysis of the H I kinematics in NGC 1532, we assumed that the disk of the galaxy is circular and contains matter concentrated in a thin disk. We assumed that the velocity versus distance from the galactic center has the form given by Brandt (1960) as

$$\frac{v(r)}{v_M} = \frac{r/r_M}{[1/3 + 2/3(r/r_M)^n]^{3/2n}}, \quad (1)$$

where r is the distance from the galaxy center and v is the circular orbital velocity. There are three parameters which fit the rotation curve: The radius r_M associated with the maximum velocity v_M, and the index n of the rotation curve. The total mass associated with this rotation curve is

$$M_\odot = 2.28 \times 10^5 (1.5)^{3/n} r_M v_M^2, \quad (2)$$

where r_M is in kpc and v_M is in km s^{-1}.

Clearly, such a model is an oversimplification. NGC 1532 may have a significant warp, and there is interaction with NGC 1531. There may be large radial motion of material and there are probably several distinct mass components: a stellar disk, a spherical halo, and the H I (gaseous phase) flattened component (e.g., Gottesman, Ball, & Hunter 1984; van Albada et al. 1985; Puche & Carignan 1991). Nevertheless, the simple analysis here should be indicative of the mass distribution in the NGC 1532 system.

The observed velocity field (see Fig. 5*c*) from the H I observations was fitted to that expected with the rotation curve form in equation (1). Apart from the edge of the H I emission where the signal-to-noise ratio is low, only two small regions had anomalous velocities greater than about 20 km s^{-1} from a rotationally symmetric velocity field. One region is near NGC 1531 where perturbations in the NGC 1532 velocity field are expected. The other field is about 2′ southwest of the nucleus of NGC 1532, where an unexpected stream of H I is moving toward the observer by $\approx$100 km s^{-1} more than expected from circular motion. These two regions, about 10% of the total area, were removed for the analysis to obtain the underlying rotation curve of NGC 1532.

The best fit of the observed velocity field to a rotation curve of the form of equation (1) is shown in Figure 6. The plotted points show the observed average velocity, corrected for inclination angle, and the smooth curve gives the best fit. The values of the three fitted parameters are $v_M = 236 \pm 6$ km s^{-1}; $r_M = 86 \pm 10$ kpc (807″ ± 90″); and $n = 0.65 \pm 0.10$. The center of rotation is $\alpha = 04^h10^m09^s.2 \pm 0^s.2$, $\delta = -33°00'00'' \pm 2''$, the systemic velocity is 1200 ± 4 km s^{-1}, and the inclination of the phase of the galaxy to the sky is 74° ± 2°.

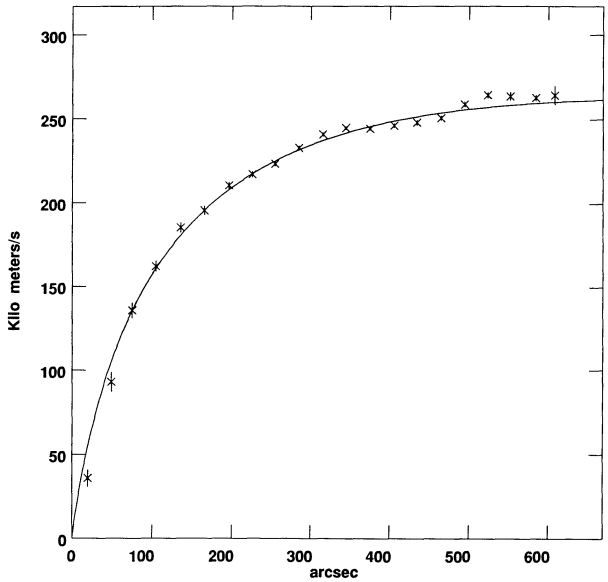

FIG. 6.—The fit of Brandt's rotation curve to the velocity field of NGC 1532. The smooth curve shows the rotation curve for the galaxy derived from the measured H I velocity field which are shown by the plotted points. These points come from Fig. 5*c*, suitably averaged over distance from the nucleus and corrected for the galaxy inclination. The assumed form and derived parameters of the rotation curve are given in the text.

5.2. *ESO 359-G29 as a Satellite of NGC 1532*

ESO 359-G29 is 760″ from the nucleus of NGC 1532, or at a projected linear separation of 82 kpc. The velocity difference between the two galaxies is 300 ± 15 km s^{-1}. Both its distance and velocity are surprisingly close to the rotation parameters determined from the H I emission in NGC 1532, extended to the distance of ESO 359-G29, and suggests that ESO 359-G29 is gravitationally bound to NGC 1532. This, in fact, was our original expectation since mixed morphological systems like ESO 359-G29 are never isolated galaxies but are associated with clusters or at the least with a dominant galaxy. However, the large velocity difference seemed to argue against association—until the above analysis of the rotation parameters of NGC 1532 was made.

The geometric configuration of ESO 359-G29 and NGC 1532 strongly constrains the projection effects. NGC 1532 is nearly on edge, i.e., its minor axis is close to the plane of the sky. Also ESO 359-G29 is nearly on the projected minor axis at a large angular distance from NGC 1532, so its true distance perpendicular to the plane is at least as great as 82 kpc, which is already quite large. Because the observed velocity difference itself is so large, it is clear that ESO 359-G29 must have the major part of its motion toward us. Thus, its velocity and location, as well as the rotational properties of NGC 1532 deduced from the H I observations, imply that ESO 359-G29 is in polar orbit around NGC 1532.

No H I was detected at the position of IC 2401, the elliptical galaxy which is 6′ ENE of the center of NGC 1532 (elliptical object in Fig. 5*a*; no H I emission at this location from Fig. 5*b*). Either its redshift is outside of the observing window (i.e., a velocity more than 300 km s^{-1} displaced from that of NGC 1532), or it has an undetected H I content. Without a redshift, this galaxy cannot be used as a probe of the gravitational field of NGC 1532. Its optical morphology is normal for a dwarf elliptical.

5.3. *The Mass-Distribution in NGC 1532*

The total mass in the NGC 1532/31 galactic system can be inferred from the rotation curve. As with all such mass estimates, the largest uncertainty in the total mass comes from our ignorance of the density of matter *beyond* where the velocity field has been measured. For example, the total mass associated with the Brandt model in Figure 6 (all of the mass was assumed to be from a thin disk) is $8.8 \times 10^{12}\ M_\odot$. The small value of $n = 0.65$ means that the rotation curve slowly decreases only beyond the location of the maximum velocity and this implies that 80% of the mass of the galaxy still lies outside of the $r_M = 88$ kpc radius. However, observations of H I in massive galaxies and binary systems (e.g., van Moorsel 1982; Gottesman et al. 1984) suggest that the radius of halos rarely exceed 50 kpc. Furthermore, the analysis assumes no significant radial motion of material, no warping of the mass distribution and only a one-component distribution of matter. Nevertheless, the following simple analysis is still indicative of the mass of the galaxy system.

The total mass within a given radius r, with the assumptions discussed in the previous paragraph, is given by rv^2/G. Using the outer part of the H I rotation curve with $v = 260$ km s^{-1} and $r = 65$ kpc (to the limit measured in Fig. 6), a mass of $1.0 \times 10^{12}\ M_\odot$ is obtained. The best "fit" of the rotation curve of equation (1), assuming an index of $n = 1.5$, a value consistent with other well-studied galaxies (e.g., Gottesman et al. 1984), gives a model with $v_M = 270$ km s^{-1} at $r = 300''$ and a total mass of $1.2 \times 10^{12}\ M_\odot$.

The predicted velocity at the location of ESO 359-G29 using the best-fit $n = 1.5$ model is only about 220 km s^{-1} and suggests that this model does not contain all of the mass associated with NGC 1532. Using the orbital elements of ESO 359-G29 with $v = 300$ km s^{-1} and $r = 82$ kpc (we are assuming a circular orbit with no projection effects), a mass of $1.7 \times 10^{12}\ M_\odot$ is calculated inside a radius of 82 kpc. This is in relatively good agreement with the estimate based on the H I rotation curve in NGC 1532 in the above paragraph. A more detailed analysis of the use of satellite galaxies as probes of the mass distribution within the group has been given by Little & Tremaine (1987).

We conclude that the total mass in the NGC 1532/31 system is $1.7 \times 10^{12}\ M_\odot$. It could be larger if ESO 359-G29 is not in a circular orbit and if the halo extends beyond 80 kpc from NGC 1532. On the other hand, if there are large noncircular motions of material in the galaxy and the warping of the stellar and H I disks is large, the total mass could be somewhat overestimated. However, the rough agreement of mass using the rotation curve of NGC 1532 and the presumed orbital motion of ESO 359-G29 suggest that the mass estimate is reasonable.

We suggest that the halo radius is about 70 kpc. The estimated mass within 65 kpc of the galaxy determined by the H I rotation curve is about $1.2 \times 10^{12}\ M_\odot$. The total mass within 82 kpc of the galaxy, inferred from the orbital elements of ESO 359-G29, is $1.7 \times 10^{12}\ M_\odot$. Within the uncertainties of the models, there appears to be little mass in the halo more than 70 kpc from the center of NGC 1532.

Using the absolute magnitude of NGC 1532 $M_{B(T)} = -21.0$ (from RSA), we obtain an integrated luminosity of $L_B = 4.0 \times 10^{10}\ L_\odot$. Thus, the mass-to-light ratio for NGC 1532 is $M_T/L_B \gtrsim 40$.

The mass in the disk component alone can be more readily determined. The disk radius (see Fig. 2*a*) is 165″ (17.7 kpc), and the rotation velocity is 200 km s^{-1} at this distance (Fig. 6). This gives a mass within a radius of 17.7 kpc of $1.6 \times 10^{11}\ M_\odot$, which is less than 10% of the total mass of the galaxy. Not all of this material within 17.7 kpc is associated with the disk component, and estimates suggest that 30% to 70% of the total mass could be in a spheroidal component (e.g., van Albada et al. 1985). Thus, the mass of the disk component falls in the range of $(0.6\text{–}1.5) \times 10^{11}\ M_\odot$.

In § 3.3 we showed that the total H I mass in NGC 1532 was $2.7 \times 10^{10}\ M_\odot$ and extends out from the galaxy center about 65 kpc, well beyond the optical disk. Within the disk we estimate that the H I mass is about 10% of the total mass.

Approximately 60% ± 10% of the total light emanates from the disk within a semimajor axis of 165″. Thus, the mass-to-light ratio, M_d/L_d, *for the disk* lies within the range of 2.5–7. This value is consistent with the ratio measured for other spiral galaxies, including the Milky Way.

The mass in the halo of NGC 1532 (the total mass minus the disk mass) is uncertain because the total mass content is uncertain. The maximum halo light L_h is $1.6 \times 10^{10}\ L_\odot$ and the minimum halo mass is M_h is $1.3 \times 10^{12}\ M_\odot$. Hence $M_{(h)}/L_{(h)} \gtrsim 80$ and could be as large as 200.

6. CONCLUSIONS

6.1. *The Nature of ESO 359-G29*

1. The optical morphology of ESO 359-G29 in the yellow and red is that of a nucleated dwarf E or dS0 galaxy, similar to those found in Virgo, Fornax, and Coma Clusters, in the rich and sparse groups, and as companions to single massive parents.

2. The optical morphology in the blue shows a small rate of recent star formation. The unusual feature is the unresolved bright nucleus at $B = 19$ ($M_B = -13$), generally absent in Sm and Im galaxies but common in dE and dS0 galaxies of total luminosity $M_{B(T)} = -17$.

3. The H I content of ESO 359-G29 is normal in all comparisons with the unbiased distance-limited sample of Virgo Cluster dwarfs (HHSS). There is no evidence for gas depletion of ESO 359-G29 as there is for the similar mixed morphology dwarf NGC 4286, which is a more extreme case of morphological mixing, both in the optical images and the radio properties.

4. The mass-to-light ratio of ~2 shows that the little dark matter is contained in this predominantly old stellar system which nevertheless contains a relatively moderate amount of hydrogen despite its mixed morphology. The dE,N morphology in the yellow and red indicating only a small present star formation rate, plus the high H I content, suggests that ESO 359-G29 is in a resting state, having not yet used up its cool hydrogen either by star formation or by outgassing.

5. ESO 359-G29 is almost certainly a companion to NGC 1532 and in a polar orbit around it (see below).

6.2. *The Halo of NGC 1532*

1. The H I emission from NGC 1532 extends 60 kpc south and 40 kpc north of the center of the galaxy and extends nearly 4 times the radius of the galaxy disk. The total H I mass is $2.7 \times 10^{10}\ M_\odot$.

2. The rotation curve, determined from the H I emission, extends over 10′ (64 kpc) radius from the galaxy. The rotational velocity at that distance is about 250 km s^{-1} and is still slowly increasing with distance. The mass estimate from the rotation curve is $1.2 \times 10^{12}\ M_\odot$ and the halo radius about 60 kpc.

3. The juxtaposition of NGC 1532 and ESO 359-G29 shows that ESO 359-G29 lies near the minor axis of NGC 1532, about 82 kpc away. At this distance its velocity is consistent with that due to rotation around the galaxy, as extrapolated from the measured H I rotation curve, again suggesting that ESO 359-G29 is in a polar orbit around NGC 1532.

4. From the assumed orbital parameters of ESO 359-G29, the total mass of NGC 1532 is $1.7 \times 10^{12} M_{\odot}$ with a radius of 82 kpc. Because this mass estimate is only slightly more than that using the H I rotation curve, we suggest that the halo radius around NGC 1532 is not larger than about 70 kpc. The total mass in NGC 1532 and the extent of the halo are in good agreement with other galaxies which have been well studied (e.g., Puche & Carignan 1991).

5. The mass-to-light ratio for the entire galaxy is about 40. The disk component has a mass-to-light ratio in the range 2.5–7.

6. The halo component has a mass-to-light ratio of at least 80.

We thank the VLA staff for giving us observing time at short notice and for their help in the reduction of data. We also thank Daniel Puche for valuable comments on the interpretation of the rotation curves.

REFERENCES

Binggeli, B., Sandage, A., & Tammann, G. A. 1985, AJ, 90, 1681
Binggeli, B., Sandage, A., & Tarenghi, M. 1984, AJ, 89, 64
Bottinelli, L., Gouguenheim, L., Fouque, P., & Paturel, G. 1990, A&AS, 82, 391
Brandt, J. C. 1960, ApJ, 131, 293
Caldwell, N. 1983, AJ, 88, 804
Carignan, C., Demers, S., & Côté, S. 1991, ApJ, 381, L13
Condon, J. J. 1989, ApJ, 338, 13
Cornwell, T. J., & Evans, K. F. 1985, A&A, 143, 77
Ferguson, H. C. 1989, AJ, 98, 367
Ferguson, H. C., & Sandage, A. 1988, AJ, 96, 1520
———. 1990, AJ, 100, 1
Fomalont, E. B., & Kristian, J. 1993, in preparation
Gottesman, S. T., Ball, R., & Hunter, J. H., Jr. 1984, ApJ, 286, 471
Haynes, M. P., Herter, T., Barton, A. S., & Benensohn, J. S. 1990, AJ, 99, 1740 (HHBB)
Hoffman, G. L., Helou, G., Salpeter, E. E., & Sandage, A. 1985, ApJ, 289, L15
Huchtmeier, W. K., & Richter, O.-G. 1989, A General Catalog of H I Observations of Galaxies (Berlin: Springer-Verlag)
Lauberts, A. 1982, The ESO/Uppsala Survey of the ESO(B) Atlas: ESO
Lauberts, A., & Valentijn, E. A. 1989, Surface Photometry Catalog of the ESO-Uppsala Galaxies: ESO
Lewis, B. M. 1987, ApJS, 63, 515
Little, B., & Tremaine, S. 1987, ApJ, 320, 493
Meurer, G. H., Freeman, K. C., & Dopita, M. A. 1988, Ap. Space Sci., 156, 141
Meurer, G. H., Freeman, K. C., Dopita, M. A., & Cacciari, C. 1992, AJ, 103, 60
Puche, D., & Carignan, C. 1991, ApJ, 378, 487
Reaves, G. 1956, AJ, 61, 69
Sandage, A., & Bedke, J. 1993, Carnegie Atlas of Galaxies (Washington, D.C.: Carnegie Institution of Washington)
Sandage, A., & Binggeli, B. 1984, AJ, 89, 919
Sandage, A., & Hoffman, G. L. 1991, ApJ, 379, L45
Sandage, A., & Perelmuter, J.-M. 1990, ApJ, 361, 1
Sandage, A., & Tammann, G. A. 1987, A Revised Shapley-Ames Catalog of Bright Galaxies (2d ed.; Washington, D.C.: Carnegie Institution of Washington)
Thompson, L. A., & Gregory, S. A. 1992, AJ, in press
Vader, J. P., & Sandage, A. 1991, ApJ, 379, L1
van Albada, T. S., Bahcall, J. N., Begeman, K., & Sancisi, R. 1985, ApJ, 295, 305
van Moorsel, G. A. 1982, Ph.D. thesis, Rijksuniversiteit, Groningen